Research Article | Vol. 8, No. 12 | 1 Dec 2018 | OPTICAL MATERIALS EXPRESS 3910
Optical Materials EXPRESS

Comparative study of praseodymium additives in active selenide chalcogenide optical fibers

ZHUOQI TANG,[1,3] LUKASZ SOJKA,[1,2] DAVID FURNISS,[1] JOEL NUNES,[1] HESHAM SAKR,[1] EMMA BARNEY,[1] SLAWOMIR SUJECKI,[1,2] TREVOR M. BENSON,[1] AND ANGELA B. SEDDON[1,4]

[1]*Mid-Infrared Photonics Group, George Green Institute for Electromagnetics Research, Faculty of Engineering, University of Nottingham, University Park, Nottingham NG7 2RD, UK*
[2]*Department of Telecommunications and Teleinformatics, Faculty of Electronics, Wroclaw University of Science and Technology, Wybrzeze Wyspianskiego 27, 50-370 Wroclaw, Poland*
[3]*zhuoqi.tang@nottingham.ac.uk*
[4]*angela.seddon@nottingham.ac.uk*

Abstract: The choice of rare earth additive when doping chalcogenide glasses can affect their mid-infrared fiber performance. Three praseodymium additives, Pr-foil, $PrCl_3$ and PrI_3 are investigated in Ge-As-Ga-Se fibers. All the fibers are X-ray amorphous and the Pr(foil)-doped fiber has the lowest overall optical loss. Pumping at 1550 nm wavelength, the Pr^{3+}-doped fibers exhibit photoluminescence across a 3.5 to 6 µm span; photoluminescence lifetimes are 10 ms for $^3H_5 \rightarrow {}^3H_4$ and 2-3 ms for ($^3H_6$, $^3F_2$)$\rightarrow {}^3H_5$ transitions. A fast 0.21 ms decay for ($^3F_3$, $^3F_4$)$\rightarrow {}^3H_6$ is observed only in the $PrCl_3$-doped fiber due to a lower phonon energy local environment of Pr^{3+} ions.

1. Introduction

Rare earth (RE) ion doped chalcogenide glasses exhibit discrete emissions across the mid-infrared (MIR) window, giving potential applications as active photonic devices like MIR amplifiers [1,2] and MIR molecular sensors [3–5] and, especially, they are the most promising materials proposed for achieving the first MIR fiber laser to work beyond 4 µm wavelength [6–9]. Although much numerical and analytical modeling work demonstrates the feasibility of MIR lasing in RE-ion-doped fibers with chalcogenide glass hosts [10–13], loss-inducing impurities and crystallization can negatively affect the quality of the fabricated RE-ion-doped chalcogenide glasses [14–17] and therefore impede realization of MIR fiber lasing. The type of RE additive used to produce the RE-ion-doping can have an important influence on chalcogenide glass-quality (*e.g.* crystallization, optical loss) [18].

RE additive in its elemental form, usually as a metallic foil, is a popular additive in the fabrication of RE-ion-doped chalcogenide bulk glass and fiber [19–21]. For example, in 2008, Park *et al* [20]. used a praseodymium metal additive to make Pr^{3+}-doped Ge-Ga-Sb-Se bulk glasses and fibers and reported spectroscopy across the 3.5-5.5 µm wavelength range. In 2015, Zhang *et al* [21]. presented the thermal and optical properties of Dy^{3+}-doped Ga-Sb-S glasses, made by adding Dy-foil during chalcogenide glass melting. In our previous research [18], both Dy foil and $DyCl_3$ additives were found to cause corrosion of the silica-glass ampoule containment during melting of Dy^{3+}-doped Ge-As-Ga-Se glasses; however the Dy^{3+}-doped Ge-As-Ga-Se glass made by Dy-foil addition led to better results of lowered scattering loss and crystallization and improved glass surface quality. $DyCl_3$ addition did not give good results at higher dopant concentrations *i.e.* ≥ 1000 ppmw Dy^{3+} [16,22]. Nevertheless, using the $DyCl_3$ additive enabled an optical loss of 1.16 dB/m at 6.6 µm wavelength in a 500 ppmw (*parts per million by weight*) Dy^{3+}($DyCl_3$)-doped Ge-As-Ga-Se fiber, without extra glass distillation and

#341552 https://doi.org/10.1364/OME.8.003910
Journal © 2018 Received 8 Aug 2018; revised 28 Sep 2018; accepted 3 Oct 2018; published 27 Nov 2018

Optical Materials EXPRESS

was purified only by heating the precursors As and Se to release their volatile oxides *etc* [23]. It is suggested that the Cl from $RECl_3$ addition can carry out reactive-gettering to remove hydrogen to reduce hydrogen-containing impurities (*e.g.* –[Se-H], -[O-H]) and so reduce the extrinsic absorption loss, *e.g.*:

$$\begin{array}{c} | \\ Se \\ | \\ H-Se-Ge-Se- \\ | \\ Se \\ | \end{array} + Cl^- \rightarrow HCl_{(g)}\uparrow + \begin{array}{c} | \\ Se \\ | \\ -Se-Ge-Se- \\ | \\ Se \\ | \end{array} \quad (1)$$

In addition, the REI_3 additive attracts interest as chalcogenide-iodine distillation and glass-melting at lower temperature have been reported [24,25]. In 2016, a Pr^{3+}-doped Ge-As-Se-In-I fiber with a minimum loss of 0.58 dB/m at 2.72 μm wavelength was presented by Karaksina *et al* [26]. Then in 2017, Shiryaev *et al*. reported a Ge-Sb-Se-In-I glass with < 0.1 ppmw, and < 0.5 ppmw, of –[H], and -[O]-, impurities, respectively [9], as a potential host for RE-ion-doping. Besides, the distillation of gallium iodide was applied to purify gallium in the fabrication of Pr^{3+}-doped Ge-As(Sb)-Ga-Se glasses/fibers [27–29]. On the other hand, iodine was reported to induce crystallization and lower photoluminescence (PL) intensity in Dy^{3+}-doped Ge-Sb-S-I glasses [30]. Also, we have observed that Ge-S-I glasses undergo chemical break down during ambient storage of a few years. To the best of our knowledge, REI_3-doped chalcogenide glass fiber has not been reported yet.

In aspect of glass system, Pr^{3+}-doped Ge-As-Ga-Se glass fibers are popularly suggested as active photonic components in the field. Recently, proposed Pr^{3+}-doped Ge-As-Ga-Se MIR fiber lasers operating at 4.5 μm [31], 4.8 μm [32] and 5.0 μm [29] wavelengths have been modeled; MIR fiber amplifiers based on Pr^{3+}-doped Ge-As-Ga-Se glasses have been simulated for amplification of signal in the range of 4-5 μm wavelength [1,2]. Therefore, in this work, the effect of Pr additives on the glass formation and optical characterization of Ge-As-Ga-Se fibers are comparatively studied for the first time, with the selected Pr-foil, $PrCl_3$ and PrI_3 dopants. The Pr^{3+}-doped Ge-As-Ga-Se fibers were investigated for amorphicity using X-ray diffraction. The transmission spectra of the fiber preform glasses were studied by Fourier transform infrared spectroscopy (FTIR) and this was engaged to analyze the historical glass quality prior to being fibers. Moreover, the optical loss, MIR PL spectra and MIR PL lifetimes of the Pr^{3+}-doped Ge-As-Ga-Se fibers were explored in the work.

2. Experimental

2.1 Glass melting and fiber fabrication

100 g total of Ge (5N, Cerac), As (7N, Furukawa Denshi; purified by heating at 310 °C for 1.5 h under a vacuum of 10^{-3} Pa) and Se (5N, Materion; purified by heating at 270 °C for 1 h 40 mins under a vacuum of 10^{-3} Pa) were melted at 850 °C for 12 hours, in the presence of a 1000 ppmw $TeCl_4$ getter (5N, Alfa Aesar) inside a silica-glass ampoule (< 0.1 ppm OH, ID/OD (inner/outer diameter) = 29/32 mm, MultiLab), then quenched and annealed at the glass transition temperature (T_g, ~240 °C). The as-annealed Ge-As-Se glass was removed from the silica-glass ampoule melting-containment inside a glovebox (≤ 0.1 ppm O_2, ≤ 0.1 ppm H_2O; MBraun) and then batched with 500 ppmw Al (5N, Alfa Aesar) into a silica-glass, bespoke distillation rig (Multilab), and a single distillation was carried out under vacuum (10^{-3} Pa). Then the distilled Ge-As-Se was melted again at 800 °C for 7 hours, quenched and annealed. The as-annealed Ge-As-Se glass was crushed into small chunks inside the MBraun glovebox

Optical Materials EXPRESS

and was either re-batched as reference glass, or re-batched with Ga (5N, Testbourne) and the praseodymium additive of: Pr foil (3N, Alfa Aesar) or $PrCl_3$ (4N, Alfa Aesar) or PrI_3 (3N, Alfa Aesar) into a fresh silica glass ampoule of ID = 8 mm, which was sealed under vacuum (10^{-3} Pa). The purity of each of the Pr additives used was the highest one available from international commercial chemical companies, including Alfa Aesar and Sigma Aldrich. The ampoule containing pre-melted Ge-As-Se glass, Ga or Pr-additive was raised to 850 °C and held isothermally for 6 hours whilst rocking ± 30 ° about a horizontal axis to homogenize the glass-melt. The chalcogenide glass melt was then quenched and annealed *in situ,* inside the silica-glass ampoule melt containment to form a rod of either: (i) $Ge_{15}As_{21}Se_{63}$ glass; (ii) 500 ppmw Pr(foil)-doped $Ge_{15}As_{21}Ga_1Se_{63}$ glass; (iii) 500 ppmw $Pr^{3+}(PrI_3)$-doped $Ge_{15}As_{21}Ga_1Se_{63}$ glass and (iv) 500 ppmw $Pr^{3+}(PrCl_3)$-doped $Ge_{15}As_{21}Ga_1Se_{63}$ glass. The host glass was the 1 at.% Ga content glass developed as in [33]. The $Pr^{3+}(PrI_3)$-doped Ge-As-Ga_1-Se glass experienced another re-melt (6 hours at 850 °C) because the glass rod preform had fractured inside the silica ampoule after the first glass-melting. Photographs of the Pr^{3+}-doped Ge-As-Ga_1-Se glass rod preforms are presented in Fig. 1; no distinct surface corrosion can be observed on any of the glass surfaces. The preforms were fiber-drawn into 230 µm diameter unstructured fibers on a customized Heathway fiber-drawing tower under N_2 ('white-spot', BOC). In this work, Ga was added to the host glass because it helped solubilize rare earth ions in chalcogenide glass matrix and is generally accepted to complex to the rare earth ions in the glass matrix [34-36]. However, the very low vapor pressure of Ga means it cannot be purified together with the Ge, As and Se in the distillation process [28], Therefore, the distilled Ge-As-Se glass/fiber rather than the Ge-As-Ga-Se host, was fabricated as the reference glass/fiber for optical loss comparison. Note that all the silica glass ampoules were pre-cleaned in $HF_{aqueous}$ and were treated for 6 hours each at 1000 °C, first in air and then under vacuum (10^{-3} Pa). Key information on glass preparation and fiber fabrication is summarized in Table 1.

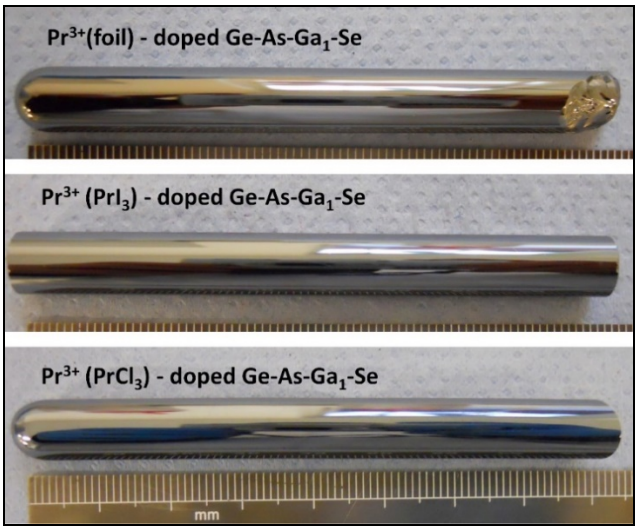

Fig. 1. Rod preforms of 500 ppmw Pr^{3+}(foil), $Pr^{3+}(PrI_3)$ and $Pr^{3+}(PrCl_3)$-doped Ge-As-Ga_1-Se glasses, showing excellent surface quality without distinct (contamination) spots (*cf* [15,16].).

Optical Materials EXPRESS

Table 1. Key information on glass preparation and fiber fabrication of 500 ppmw Pr^{3+}(foil), Pr^{3+}(PrI_3) and Pr^{3+}($PrCl_3$)-doped Ge-As-Ga_1-Se glass fibers and the Ge-As-Se fiber. (Note N is nines' purity.)

Host glass	$Ge_{15}As_{21}Se_{63}$ + Ga_1	$Ge_{15}As_{21}Se_{63}$ + Ga_1	$Ge_{15}As_{21}Se_{63}$ + Ga_1	$Ge_{15}As_{21}Se_{63}$
Pr concentration	500 ppmw	500 ppmw	500 ppmw	n.a.
Pr additives	Pr foil	PrI_3	$PrCl_3$	
Pr additive purity and source	3N, Alfa Aesar	3N, Alfa Aesar	4N, Alfa Aesar	
Preform remelt (after batching of Pr additive)	6 hours @ 850°C	2 × 6 hours @ 850°C	6 hours @ 850°C	6 hours @ 850°C
Host precursor purity and source	Ge: 5N, Cerac; As: 7N, Furakawa Denshi; Se: 5N, Materion; Ga: 5N, Testbourne			
Fiber details	230 μm diameter, unstructured			

2.2 Characterization of bulk glass and fiber

Powder XRD patterns of each fiber were collected using a Siemens D500 system, running from 10 °2θ to 70 °2θ at step-size 0.05 °2θ *per* 40 seconds, totaling >12 hours for each XRD run. In fiber loss measurement, the two-groups-cleaves' cut-back method [37] was applied with a IFS 66/S, Bruker FTIR spectrometer. Then for FTIR spectroscopy of bulk glass, using the same spectrometer, bulk sample disks were sawn from the glass preforms prior to fiber drawing. All the FTIR samples were placed together on a copper sample holder for a multi-samples' polishing protocol to a 1 μm finish on the opposite parallel faces of the discs, in order to approach the same polishing quality for comparison of baseline losses. The thickness of the FTIR samples was 2.771 ± 0.005 mm.

Fiber PL spectra of the Pr^{3+}-doped Ge-As-Ga_1-Se samples were collected using a pump laser at 1550 nm (FPL 1009S, Thorlabs), a monochromator (MiniMate, Spex), a lock-in amplifier (7270 DSP, Metek) and an ambient MCT detector (mercury-cadmium-telluride, PVI-6, Vigo System). As shown in Fig. 2(a), the set-up was fiber side-collection of PL intensity. In fiber PL lifetime measurements, the 1550 nm pump laser (Thorlabs) was modulated at 6.4 Hz, and used along with the monochromator (Spex), an electric-cooled MCT detector (PVI-4T-6, Vigo System) and a digital oscilloscope (Picoscope5204, Pico Technology) for the collection of fluorescent decay. As shown in Fig. 2(b), the PL lifetimes were also measured using fiber side-collection. The accuracy of a wavelength selected and measured by the monochromator system was ± 20 nm. Both fiber PL spectra and lifetimes were collected from the side of the cleaved fibers, specifically in order to minimize re-absorption [38,39] and any influence of optical loss. In this set-up, there was very short optical pathlength for the emitted light to leave the side of fiber, which had a diameter of 230 μm. Also, an effective 2 mm length of the fiber sample was used in the PL signal collection (each fiber sample was 117 mm total length but this length was mainly used for the purpose of holding the sample on a V-groove holder; the 2 mm fiber length sticking out of the sample holder was actually used for the PL collection). Also, in this side collection, a 2945 nm wavelength long-pass filter (Northumbria Optical Coatings) was applied between the fiber and monochromator to prevent any high orders of scattered light from the pump from affecting the monochromator measurements; the $PrCl_3$-doped fiber and the PrI_3-doped fiber exhibited a high scattering loss at the 1550 nm wavelength of the pump laser, whereas the Pr(foil)-doped fiber did not present distinct scattering loss at this wavelength. The system response was measured using a Globar blackbody source and all of the PL spectra in this work were corrected for this. In the measurement of PL lifetime, each presented decay plot was collected from one fiber sample with the same alignment and was measured for up to 14000 times to improve the signal-to-noise ratio. In lifetime calculation, for comparatively long transitions of >1 ms in $^3H_5 \rightarrow {}^3H_4$ and $(^3H_6, {}^3F_2) \rightarrow {}^3H_5$, the fitting error was ~0.2 ms for the Pr^{3+}(foil) and Pr^{3+}(PrI_3)-doped fibers, and the error increased to ~0.7 ms for the Pr^{3+}($PrCl_3$)-doped fiber due

Optical Materials EXPRESS

to less signal and more noisy PL decay. For <1 ms short transition of $(^3F_3, {}^3F_4)\rightarrow{}^3H_6$, the fitting error of calculated lifetime was 0.06 ms with the $Pr^{3+}(PrCl_3)$-doped fiber.

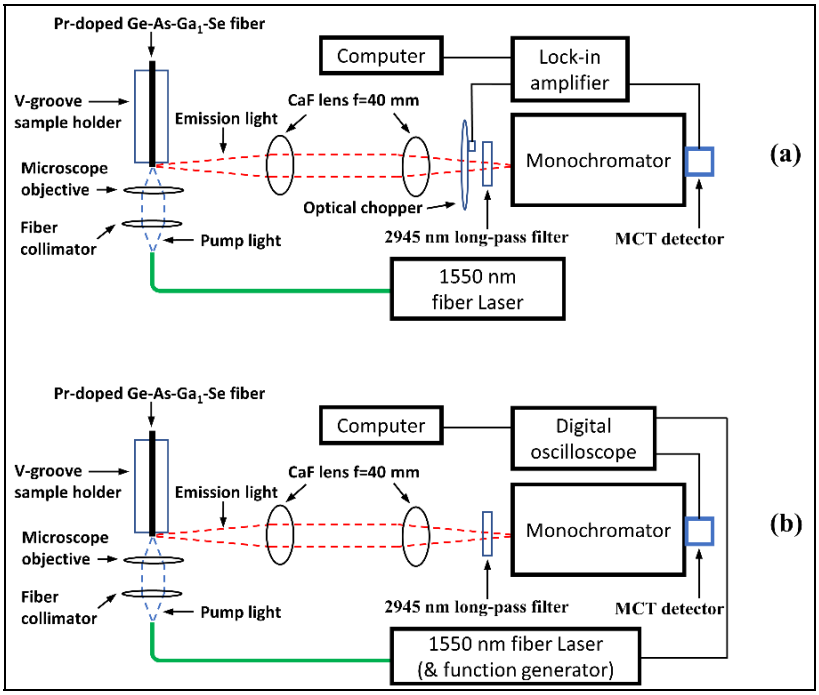

Fig. 2. Set-up for measurement of the Pr^{3+} -doped Ge-As-Ga_1-Se glass fibers for fiber side-collection of (a) PL spectrum and (b) PL lifetime.

3. Results and discussion

3.1 Fiber XRD, fiber loss and FTIR spectroscopy of bulk glass

Powder XRD patterns of the 500 ppmw Pr^{3+}(foil), $Pr^{3+}(PrI_3)$ and $Pr^{3+}(PrCl_3)$-doped Ge-As-Ga_1-Se fibers are presented in Fig. 3 and all of them indicate XRD amorphicity. In our previous work, 500 ppmw $Dy^{3+}(DyCl_3)$-doped Ge-As-Ga_3-Se glass fiber exhibited a small amount of crystallization to a modified α-Ga_2Se_3 [23]. In this work, the XRD pattern of the 500 ppmw $Pr^{3+}(PrCl_3)$-doped Ge-As-Ga_1-Se glass fiber did not present any distinct crystallization peaks. Although the rare-earth ion chloride additive was different ($PrCl_3$ instead $DyCl_3$), it is believed that lowering the Ga content from 3 at% to 1 at% played an important role in reducing crystals in the Ge-As-Ga-Se fiber. This is supported by our previous study that lowering Ga content helped decrease Ga_2Se_3 crystals in 3 at % Ga compared to 10 at % Ga additive in Ge-As-Ga-Se bulk glasses [15].

Figure 4 shows optical loss spectra of the 500 ppmw Pr^{3+}(foil), $Pr^{3+}(PrI_3)$ and $Pr^{3+}(PrCl_3)$-doped Ge-As-Ga_1-Se glass fibers and the Ge-As-Se fiber. For all the fibers, there were very small [H-O-H] and -[O-H] impurity bands (< 0.2 dB/m) at 3.0 μm and 6.3 μm wavelengths, respectively. Small = [As-O]- and ≡[Ge-O]- absorption bands were observed < 0.7 dB/m at about 7.8 μm wavelength. The underlying –[Se-H] vibrational absorption band centered at 4.5 μm wavelength (represents ~30 to 40 dB/m loss [40]), and the Pr^{3+} electronic absorption band in the 3.5 to 6 μm wavelength range caused the detector not to gather light for the fiber lengths (3-7 m) tested, *i.e.* overloaded absorption band.

Optical Materials EXPRESS

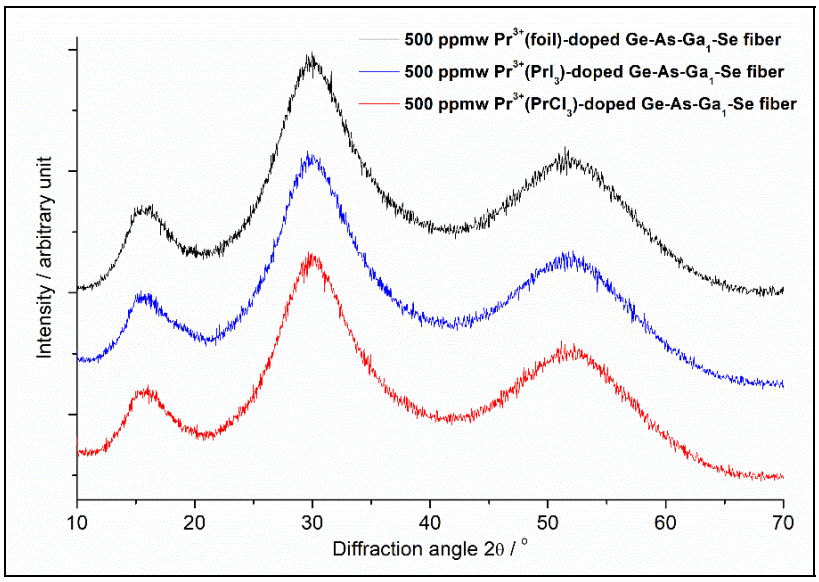

Fig. 3. Powder XRD patterns of the 500 ppmw Pr^{3+}(foil), $Pr^{3+}(PrI_3)$ and $Pr^{3+}(PrCl_3)$-doped Ge-As-Ga_1-Se glass fibers.

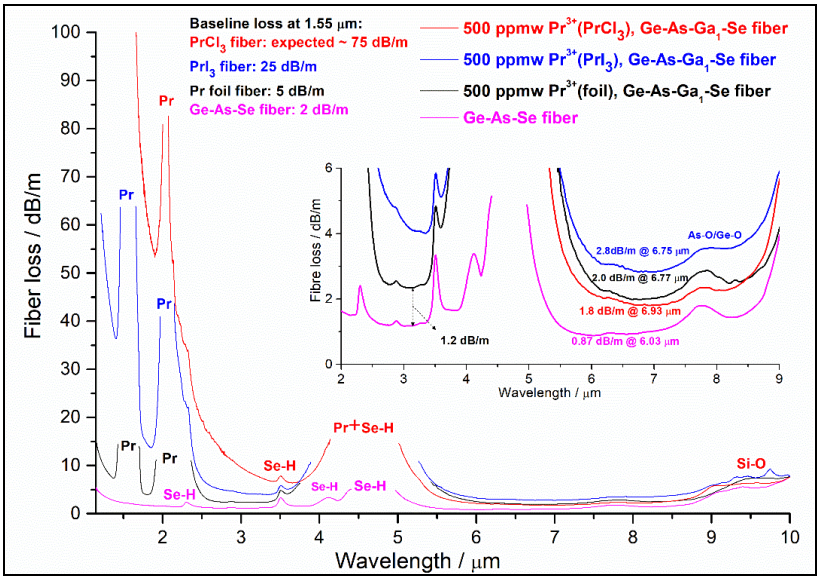

Fig. 4. Optical loss spectra of the 500 ppmw Pr^{3+}(foil), $Pr^{3+}(PrI_3)$ and $Pr^{3+}(PrCl_3)$-doped Ge-As-Ga_1-Se glass fibers and Ge-As-Se fiber. The inset shows enlarged details of the low loss for comparison.

In Fig. 4, the Ge-As-Se fiber exhibits the lowest baseline loss of 1.2-1.3 dB/m at 2.5 to 3.4 μm wavelength and 0.9 to 1.0 dB/m at 5.6-7.0 μm wavelength, and the lowest loss is 0.87 dB/m at 6.03 μm wavelength. After including the Ga solubilizer and Pr additives to make the 500 ppmw Pr^{3+}-doped Ge-As-Ga_1-Se fibers, the background optical loss increased. Both the $PrCl_3$-doped fiber and the PrI_3-doped fiber presented a clear extra scattering loss in the NIR range. Using 1.55 μm as a wavelength reference point (which was the pump wavelength for the PL results in this work), the baseline optical loss of Ge-As-Se fiber, Pr(foil)-doped fiber,

Optical Materials EXPRESS

PrI_3-doped fiber and $PrCl_3$-doped fiber increased in the order: 2 dB/m, 5 dB/m, 25 dB/m and ~75 dB/m, respectively.

Among the 500 ppmw Pr^{3+}-doped Ge-As-Ga_1-Se fibers, the Pr foil-doped fiber had the lowest overall fiber baseline loss across the 2 to 9 µm range; this was 2.0-2.5 dB/m at wavelengths of 2.7-3.4 µm and 6.0-7.5 µm. Note that, although the $PrCl_3$-doped fiber exhibited a large scattering loss in the NIR region, this fiber actually gave the lowest minimum loss of 1.8 dB/m at 6.93 µm wavelength amongst all of the RE-ion-doped-fibers here (see inset of Fig. 4). Finally, the PrI_3-doped fiber presented the highest baseline loss (3 dB/m) above 6 µm wavelength. Further analysis of fiber loss was assisted by FTIR results of fiber preform glass as follows.

FTIR spectra of bulk glass samples cut and polished from the as-prepared rod-preforms before fiber-drawing of the 500 ppmw Pr^{3+}(foil), Pr^{3+}(PrI_3) and Pr^{3+}($PrCl_3$)-doped Ge-As-Ga_1-Se glasses and the Ge-As-Se glass are given in Fig. 5. In this work, the FTIR bulk glass samples underwent co-multi-polishing in an effort to reduce any variability of surface finish and optical path length and enhance the analysis of baseline loss comparison. As the background loss levels of the FTIR spectra of the bulk glass samples were not absolute, all spectra were vertical shifted to be overlapped in the 6 to 8 µm wavelength range to aid the comparison of any excess scattering loss in the NIR region. From Fig. 5, it is evident that both the $PrCl_3$-doped and PrI_3-doped bulk glasses exhibited excess NIR scattering loss compared to that of the Pr foil-doped bulk glass and the Ge-As-Se bulk glass which had almost overlapping baselines (also see inset (a) to Fig. 5). Adding the Ga and Pr additives is bound to change the properties of the Pr^{3+} -doped Ge-As-Ga_1-Se glasses: including density and/or dielectric constant fluctuations, in comparison to the base Ge-As-Se glass. This will contribute an associated variation in scattering loss [41]. However, the scattering loss induced by such compositional change is expected to be small (for As_2Se_3 from [41] anticipated to be within the scale of dB/km) compared to the distinct extra scattering loss found in the $PrCl_3$-doped and PrI_3-doped glasses (≥20 dB/m at 1.55 µm wavelength).

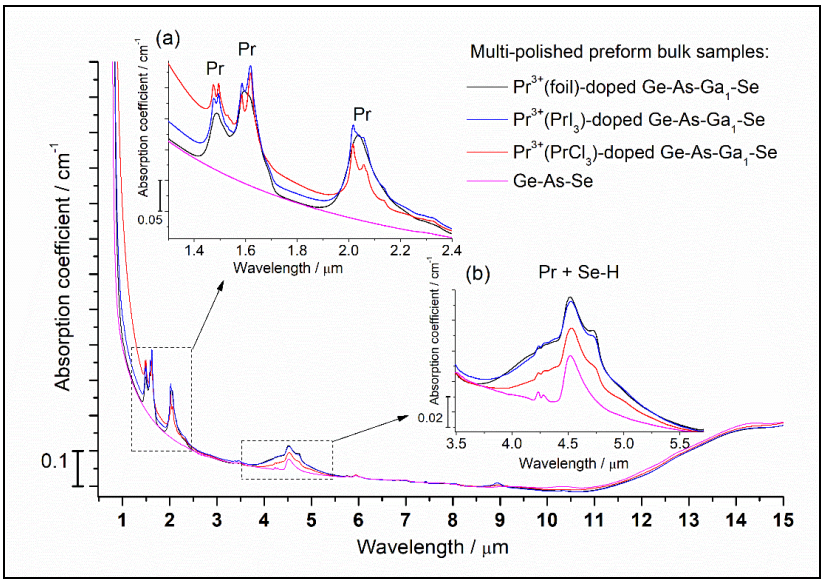

Fig. 5. FTIR spectra of as-prepared bulk glass samples cut and polished from rod-preforms prior to fiber-drawing. The bulk glasses were: 500 ppmw Pr^{3+}(foil), Pr^{3+}(PrI_3) and Pr^{3+}($PrCl_3$)-doped Ge-As-Ga_1-Se glasses and the Ge-As-Se glass. Inset (a) shows the enlarged characteristic of absorption bands at wavelengths of 1.5 µm, 1.6 µm and 2.0 µm. Inset (b) shows the enlarged absorption band at about 4.5 µm wavelength.

Optical Materials EXPRESS

Note that inset (a) of Fig. 5 shows that at 1.5 μm, 1.6 μm and 2.0 μm wavelengths, the Pr(foil)-doped bulk glass exhibited unstructured Pr^{3+} electronic absorption bands, but that the $PrCl_3$-doped and PrI_3-doped bulk glasses instead exhibited structured Pr^{3+} electronic absorption bands. This structuring is due to Stark level absorptions because of a more ordered environment and suggests that for the as-prepared PrI_3 and $PrCl_3$-doped bulk glasses, at least a part of the population of the Pr^{3+} ions did not dissolve properly in the glassy matrix environment and probably remained mainly coordinated with Cl/I instead of Se, although this does not necessarily indicate clustering. Moreover, inset (b) of Fig. 5 presents the characteristics of the absorption bands around 4.5 μm wavelength. The Ge-As-Se fiber exhibited a 0.035 cm^{-1} absorption coefficient (equivalent to 35 dB/m) due solely to a –[Se-H] vibrational absorption band centered at 4.5 μm wavelength. However, for the Pr^{3+}-doped bulk glasses, the Pr^{3+} electronic absorption band and –[Se-H] vibrational absorption band overlapped in the region around 4.5 μm wavelength; the $PrCl_3$-doped glass presented a lower overall band height compared to the Pr(foil)-doped and PrI_3-doped bulk glasses. Like in [40], the absorption band at 4.5 μm wavelength was then deconvoluted to its components viz.: vibrational absorption due to extrinsic impurity in the glass: –[Se-H], and the Pr^{3+} electronic absorption. The –[Se-H] loss was 38 dB/m, 32 dB/m and 28 dB/m, respectively, at 4.5 μm wavelength for the Pr foil-doped, $PrCl_3$-doped and PrI_3-doped fibers, respectively. From this result, we venture to suggest that the presence of chloride and iodide acted as a [H]-getter thereby reducing the extrinsic loss due to –[Se-H] impurity absorption. Also, the Pr^{3+} absorption band at ~4.5 μm wavelength was found structured in both PrI_3-doped and $PrCl_3$-doped glasses.

Combining optical losses shown in Fig. 4 and Fig. 5, there would have been refractive index discontinuities in the $PrCl_3$-doped/PrI_3-doped bulk glass and fiber that caused the large wavelength-dependent scattering loss. The possible sources of such 'refractive index discontinuities' were: (i) more structured but not yet crystallized Pr-Cl/Pr-I local environment sites (which would also contribute to the structured Pr^{3+} absorption bands in Fig. 5); (ii) the XRD technique had a ~1 to 5% volume detection limitation (depends on type of crystals), so there was possibility of a small amount of XRD-undetectable crystals caused the extra scattering loss in the $PrCl_3$/PrI_3-doped glasses; such crystals could be either Pr^{3+}-containing (e.g. $PrCl_3$/PrI_3) or formed by the host glass elements (*e.g.* Ga_2Se_3) - for example, Ge-modified α-Ga_2Se_3 crystals were found in $DyCl_3$-doped Ge-As-Ga-Se glasses in our previous work [16]; (iii) compositional fluctuation (including phase separation) in some sites of the host glass; (iv) fine Si-O/Pr-O-containing particles from rare earth ion corrosion during the chalcogenide glass melting in the silica-glass ampoule melt-containment. It is noted that the rare-earth-ion trichloride additives appear to exert stronger silica-glass ampoule corrosion than that of the rare-earth foil additive [18]. According to the Group of Churbanov, wavelength-dependent loss in the transparent window of chalcogenide glass fibers can be caused by excess scattering loss due to silica particles [42,43]. Even though, it should also be noted that in our previous work, a 500 ppmw Dy($DyCl_3$)-doped Ge-As-Ga_3-Se bulk glass and fiber did not present such distinct NIR excess scattering loss [16,23]. It is possible that $PrCl_3$ is more aggressive than $DyCl_3$ in attacking the silica-glass ampoule, although the chemistry of the rare earth ions is usually similar, being dependent on inner f-electrons and shielded by outer electrons. The presence of 3 at % Ga (rather than 1 at% Ga here) in the previous case [16,23] might have helped to solubilize the $DyCl_3$ and reduce excess scattering loss.

In addition, we discount crystallization during reheating of the glasses to draw fiber as a main cause of scattering loss in the $PrCl_3$-doped and the PrI_3-doped fibers (Fig. 4). This is because: (i) both fibers were XRD amorphous (see Fig. 3) and (ii) the same NIR scattering occurred also in the as-prepared bulk glass fiberoptic preforms prior to the fiber drawing. Inset (a) of Fig. 5, gives the absorption coefficient (i.e. total loss coefficient) of the bulk glass of the fiberoptic preform of each of the $PrCl_3$-doped and PrI_3-doped as approximately 0.06 and 0.02 cm^{-1} (corresponding to 60 and 20 dB/m), respectively, higher than that of the Pr foil-doped

Optical Materials EXPRESS

bulk glass at 1550 nm wavelength. These values of optical loss are close to that given in Fig. 4 for a comparison of the fibers: the excess loss in the $PrCl_3$-doped and PrI_3-doped fibers, are also ~70 dB/m and 20 dB/m, respectively, compared to the loss of the Pr-foil fiber at 1550 nm wavelength. Thus, it is concluded that the fiber-drawing process did not produce distinct extra crystallization over and above the fiberoptic preform to contribute to the NIR scattering loss in the $PrCl_3$-doped and PrI_3-doped fibers. However, it cannot be ruled out that there was some crystallization in the fiberoptic preforms.

We know that 500 ppmw Pr doping in a Ge-As-Ga_1-Se glass satisfies the recommended 10:1 ratio of the gallium: rare-earth in chalcogenide glass hosts [34,36]. However, in this work, we have found that only the 500 ppmw Pr foil appears to have been properly dissolved in the Ge-As-Ga_1-Se host glass system. Therefore, importantly, the results of this work indicate that the ratio of gallium: rare-earth could depend on *which* rare earth additives are to be used. According to the order of excess scattering losses discussed above, the required Ga content to solubilize the particular form of rare earth ion additive is suggested in order of: $Ga_{PrCl3} > Ga_{PrI3} > Ga_{Pr\text{-}foil}$.

3.2 Fiber photoluminescent (PL) spectra and lifetimes, and Pr^{3+} site variation

Figure 6 presents the PL spectra of the 500 ppmw Pr^{3+}(foil), Pr^{3+}($PrCl_3$) and Pr^{3+}(PrI_3)-doped Ge-As-Ga_1-Se fibers, on pumping at 1550 nm wavelength. From Fig. 5, the Pr^{3+} absorption band of the $PrCl_3$-doped chalcogenide fiber is of lower intensity than that of each of the Pr foil or PrI_3-doped fiber. It is inferred that fewer Pr^{3+} ions had successfully dissolved homogeneously in the $PrCl_3$-doped chalcogenide glass; the knock-on effect is an expected lower Pr^{3+} PL intensity for the $PrCl_3$-doped fiber than the other two fibers, which is observed in Fig. 6. The only caveat is that this assumes a constant emission cross-section across the three types of Pr^{3+} dopants. The structured shape of the Pr^{3+} absorption bands and the reduction in Pr^{3+} absorption band intensity observed in FTIR spectra of the $PrCl_3$- and PrI_3-doped glasses (see Fig. 5) indicate that there may be at least three population-types of the Pr^{3+} ions. Firstly, there are well-behaved, ideal Pr^{3+} ions which are coordinated by selenium and are bonded into the glassy network and homogeneously distributed and produce PL. Secondly there is a population of Pr^{3+} ions which contribute to the PL and which exist as Pr^{3+} $(Cl)_n$ and Pr^{3+} $(I)_n$ halide-coordinated units in the host glass, where the first coordination sphere may be partially substituted with selenium and which may be either dissolved in the glass and distributed homogeneously or these units could be more ordered and/or clustered to explain the structuring of the Pr^{3+} electronic absorption bands. The lowering of the absorption band intensity for Pr^{3+} in the $PrCl_3$-doped chalcogenide glass suggests that a third population of the praseodymium ions does not contribute to the absorption band at all, nor to the PL band, and may have precipitated out as oxide at the interface between the chalcogenide glass and the silica glass containment, as we found in our previously reported work, perhaps as oxide [18], although the preform surface was shiny under photo (see Fig. 1). The exact distribution of Pr-Cl/Pr-I/Pr-Se/Pr-O sites is unknown. It was found that the peak PL was repeatable at 4700 nm wavelength for all the three Pr^{3+} -doped Ge-As-Ga_1-Se fibers. Also, all the fiber PL spectra had dips at 4.5 μm wavelength due to –[Se-H] impurity underlying vibrational absorption and dips at 4.2 μm wavelength due to the external CO_2 absorption in the optical path of the PL set-up. There was a small PL peak found at 5750 nm wavelength in $PrCl_3$-doped fiber; although it was noisy, the observation was repeatable and could be due the lower phonon energy local environment offered by Cl coordination of Pr^{3+} which could encourage the inner, upper radiative transition: $(^3F_3, {}^3F_4) \rightarrow {}^3H_6$.

The PL intensities at 4700 nm wavelength of the 500 ppmw Pr^{3+}(foil), Pr^{3+}(PrI_3) and Pr^{3+}($PrCl_3$)-doped Ge-As-Ga_1-Se fibers are shown as a function of pump power at 1550 nm wavelength in Fig. 7. A gentle sublinear behavior was observed for all fibers. This result is probably due to ground state bleaching [44].

Optical Materials EXPRESS

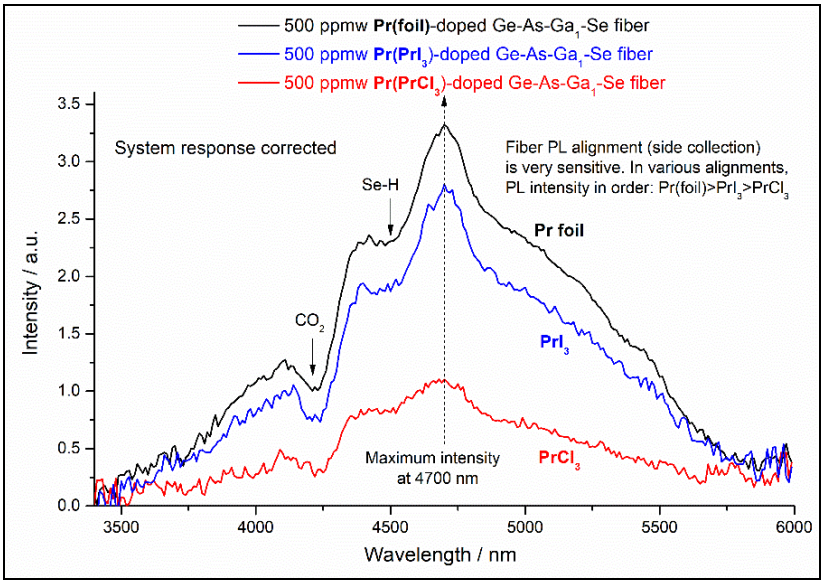

Fig. 6. Photoluminescence spectra of the 500 ppmw Pr^{3+}(foil), Pr^{3+}(PrI_3) and Pr^{3+}($PrCl_3$)-doped Ge-As-Ga_1-Se fibers, pumped at 1550 nm wavelength with 65 mW power. Fiber side collection of the PL was applied and spectra were corrected for system response.

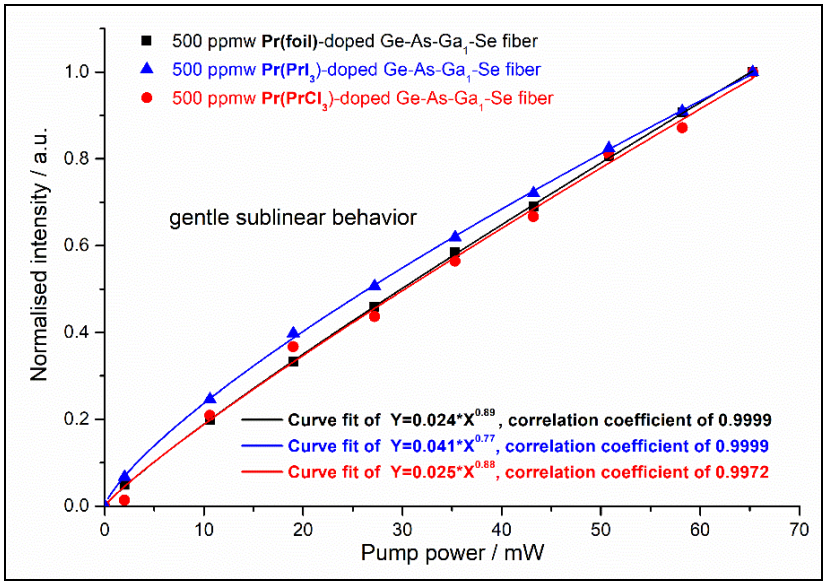

Fig. 7. Variation of the photoluminescence (PL) intensity, taken at the position of maximum intensity PL at 4700 nm wavelength, with pump power at 1550 nm wavelength, of the 500 ppmw Pr^{3+}(foil), Pr^{3+}(PrI_3) and Pr^{3+}($PrCl_3$)-doped Ge-As-Ga_1-Se fibers.

The decays of the maximum intensity PL at 4700 nm wavelength in the 500 ppmw Pr^{3+}(foil) and Pr^{3+}(PrI_3)-doped Ge-As-Ga_1-Se fibers are presented in Fig. 8. It was found that two exponential decay lifetimes were required, of 10.1 ms and 3.3 ms to fit best for Pr(foil)-doped fiber and of 10.4 ms and 3.2 ms to fit best for the Pr(PrI_3)-doped fiber. The inset of Fig. 8 of the Pr^{3+}-ion simplified energy level diagram [45–47] shows that the shorter ~3 ms lifetime was due to the transition of ($^3H_6$, $^3F_2$)→$^3H_5$ and the ~10 ms lifetime to the transition of $^3H_5$→$^3H_4$; a full energy level diagram of the Pr^{3+} ion can be found in Weber's work [48]. From

Optical Materials EXPRESS

the fitting, the contributions to the steady state PL intensity at 4700 nm wavelength of $^3H_5 \rightarrow {}^3H_4$ and ($^3H_6$, $^3F_2$)$\rightarrow {}^3H_5$ transitions were suggested to be in a ratio of roughly 3: 1 or 3.5: 1 (judged by A_n in the fit function, Fig. 8), respectively, for the Pr^{3+}(foil) or Pr^{3+}(PrI_3)-doped fiber. For all the energy level diagrams presented in this work, the wavelength(s) next to the down arrow (4.0 µm, 4.8 µm and 5.2 µm) represents the nominal peak wavelength of each potential transition band [45–47]. Due to the thermally coupled, broad energy levels of ($^3H_6$, $^3F_2$) and ($^3F_3$, $^3F_4$), the transition bands of ($^3H_6$, $^3F_2$)$\rightarrow {}^3H_5$ and ($^3F_3$, $^3F_4$)$\rightarrow {}^3H_6$ are broad and have chance to contribute to the lifetime measurement at 4700 nm wavelength [46,49].

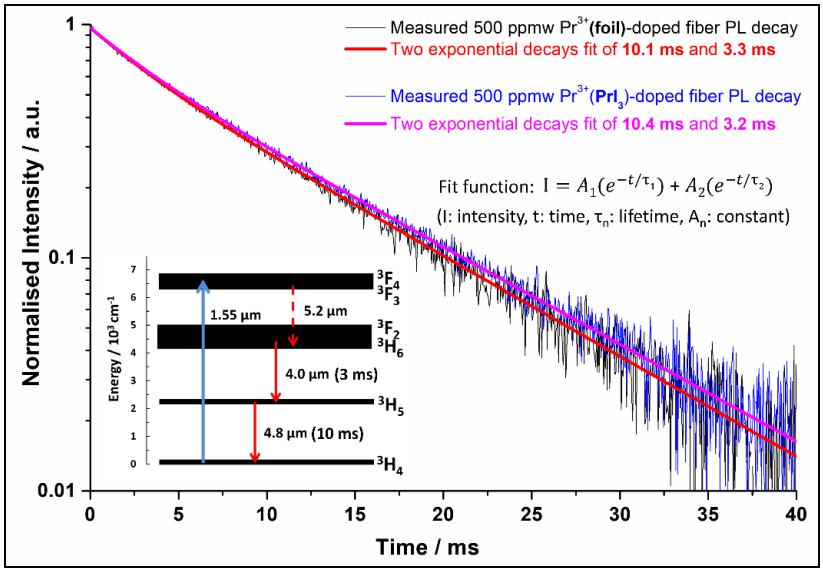

Fig. 8. PL decay and exponential fits of the 500 ppmw Pr^{3+}(foil) and Pr^{3+}(PrI_3)-doped Ge-As-Ga_1-Se fibers, at 4700 nm wavelength. Pump power was 65 mW, at 1550 nm wavelength. The inset presents the two lifetimes of 3 ms (($^3H_6$, $^3F_2$)$\rightarrow {}^3H_5$) and 10 ms ($^3H_5 \rightarrow {}^3H_4$) in a Pr^{3+}-ion simplified energy level diagram [45–47]. The wavelength of each down arrow is the peak wavelength of the potential PL band in each transition.

Figure 9 presents the PL decay of the 500 ppmw Pr^{3+}($PrCl_3$)-doped Ge-As-Ga_1-Se fiber at the 4700 nm wavelength of maximum PL intensity. In contrast to the other two doped fibers, a rapid drop in PL intensity occurred in the first 1 ms of the Pr^{3+}($PrCl_3$)-doped fiber PL decay (reproducible in the experiment), which indicates this decay region was dominated by a short lifetime. Three exponential decay lifetimes of 10.3 ms, 2.4 ms and 0.21 ms were required to best fit the PL decay of the Pr^{3+}($PrCl_3$)-doped fiber, assigned to: $^3H_5 \rightarrow {}^3H_4$, ($^3H_6$, $^3F_2$)$\rightarrow {}^3H_5$ and ($^3F_3$, $^3F_4$)$\rightarrow {}^3H_6$, respectively (see inset of Fig. 9), and it was suggested that these transitions contributed to the steady state PL intensity at 4700 nm wavelength in an approximate ratio of 4: 1: 1.3, according to the fit function (Fig. 9).

The local environments suggested for the Pr^{3+} ions facilitating PL in the Pr^{3+}($PrCl_3$)-doped Ge-As-Ga_1-Se fiber are depicted in Fig. 10. Part of the Pr^{3+} ions were coordinated with Se in local environment and when pumped at 1550 nm wavelength, the decay transitions of $^3H_5 \rightarrow {}^3H_4$ and ($^3H_6$, $^3F_2$)$\rightarrow {}^3H_5$ would be found and were observed but the ($^3F_3$, $^3F_4$)$\rightarrow {}^3H_6$ transition would have mostly decayed non-radiatively (*i.e.* same as in Pr(foil)-doped fibers). Additionally, in the Pr^{3+}($PrCl_3$)-doped fiber, as mentioned at least a portion of the Pr^{3+} ions would have had a first coordination shell of chloride ions, which may or may not have been partially substituted with Se ions. These Pr^{3+} centers may have been more ordered, may have clustered or may have formed small crystals. Nonetheless, this first coordination sphere of Cl (or Cl, Se) would have provided a local phonon energy to the Pr^{3+} ions which was much lower

Optical Materials EXPRESS

than that of a first coordination sphere of Se alone, thus mediating the upper radiative decay in $(^3F_3, {}^3F_4)\rightarrow{}^3H_6$, which made the 0.21 ms lifetime observable. The evidence to support this hypothesis is as follows.

Firstly, as discussed, the $PrCl_3$-fiber exhibited high NIR scattering loss, structured Pr^{3+} absorption bands and a much lower PL intensity centered at 4700 nm than the Pr^{3+}(foil)-doped fiber; these observations indicate that some of the $PrCl_3$ additive might not have dissolved properly in the Se-matrix (and the Pr^{3+} bonded with Cl instead). Secondly, in our previous work on $DyCl_3$-doped Ge-As-Ga_{10}-Se glasses, when the Dy^{3+} concentration was <1000 ppmw, we concluded from the extended X-Ray absorption fine structure (EXAFS) [22] and also Beer-Lambert studies that the Dy^{3+} fully had been incorporated into the glass network (Dy-Se coordination); yet when the Dy^{3+} concentration was ≥ 1000 ppmw, Dy^{3+} was shown to be in a dominantly crystalline Dy-Cl environment by the EXAFS [22]. This supports the hypothesis that a crystalline $PrCl_3$ environment was also possible in the Ge-As-Ga-Se glass system. Thirdly, lasing has been reported at 5.2 μm wavelength ($(^3F_3, {}^3F_4)\rightarrow{}^3H_6$) in a Pr^{3+}-doped $LaCl_3$ crystal [50] and the host phonon energy was reported to be 210 cm^{-1} wavenumber [51]. In other words, the Cl-coordinated Pr^{3+} local environment had very low phonon energy which would have encouraged the radiative transition of $(^3F_3, {}^3F_4)\rightarrow{}^3H_6$. As a comparison, a selenide-based chalcogenide glass is generally considered to have a phonon energy of ~350 cm^{-1}[52,53].

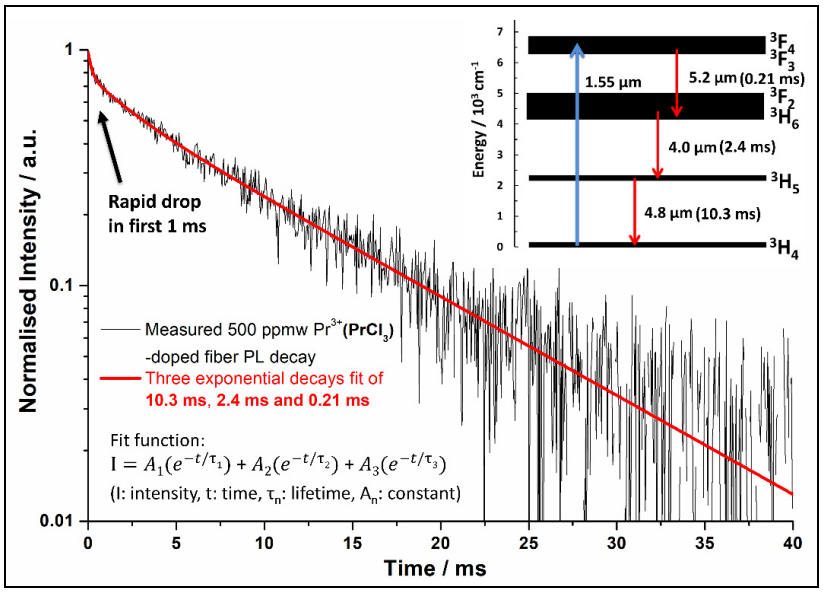

Fig. 9. PL decay and exponential fit of the 500 ppmw $Pr^{3+}(PrCl_3)$-doped Ge-As-Ga_1-Se fiber, at 4700 nm wavelength (65 mW pump power at 1550 nm wavelength). The inset presents three lifetimes of 0.21 ms ($(^3F_3, {}^3F_4)\rightarrow{}^3H_6$), 2.4 ms ($(^3H_6, {}^3F_2)\rightarrow{}^3H_5$) and 10.3 ms ($^3H_5\rightarrow{}^3H_4$) in a simplified energy level diagram of Pr^{3+}-ion [45–47].

On the other hand, such Cl-coordinated sites did not happen in the Pr^{3+}(foil)-doped fiber and so it is assumed that the selenide (and possibly oxide, hydroxide and –[Se-H]) coordination of Pr^{3+} ions offered phonons of higher energy which could bridge the $(^3F_3, {}^3F_4)\rightarrow{}^3H_6$ gap giving non-radiative decay mostly in this transition. Moreover, the $Pr^{3+}(PrI_3)$-doped glass exhibited a structured Pr^{3+} absorption band (Fig. 5), which also indicates part of the PrI_3 did not dissolve properly in a Se coordinated environment. Residual iodide coordination of Pr^{3+} in the $Pr^{3+}(PrI_3)$-doped glass would give an even lower local phonon energy than for chloride coordination and so one would expect to see again radiative decay due to $(^3F_3, {}^3F_4)\rightarrow{}^3H_6$ and the 5750 nm wavelength PL band for the $Pr^{3+}(PrI_3)$-doped fiber as for the $Pr^{3+}(PrCl_3)$-doped

Optical Materials EXPRESS

fiber. However, it is known that iodine can take up the role of a chalcogen chain terminator as in: ≡Ge-S/Se-S/Se-S/Se-I or = As-S/Se-S/Se-I *etc* [54]. and this may be the reason why iodide was less inclined to remain coordinated to Pr^{3+}. In addition, iodine is less electronegative than chlorine and so will have lowered philicity for the electropositive Pr than chlorine. Along with this, it was observed that, when compared to the $PrCl_3$-doped glass/fiber, the intensities of the Pr^{3+} absorption band and the PL band were distinctly higher in the PrI_3-doped glass/fiber (see Fig. 5 and Fig. 6). This would indicate the amount of Pr^{3+} coordinated with iodide in the local environment was much less and Pr-Se sites were greater in number in PrI_3-doped fiber (compared to Pr-Cl in the $PrCl_3$-doped fiber). A smaller quantity of Pr-I sites would not allow the experimental observation of the extra lifetime of ($^3F_3$, $^3F_4$)→$^3H_6$ and the 5750 nm wavelength PL band in the PrI_3-doped fiber.

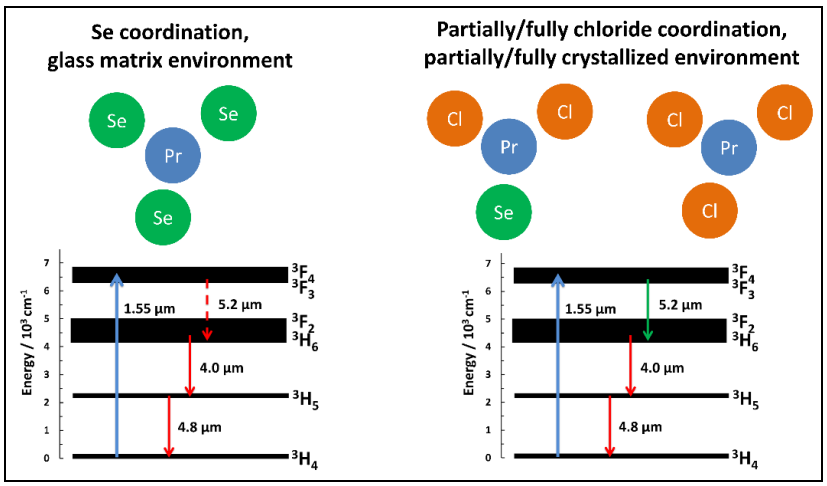

Fig. 10. Schematic diagram of the proposed candidate environments of Pr^{3+} ion facilitating PL in the 500 ppmw Pr^{3+}($PrCl_3$)-doped Ge-As-Ga_1-Se fiber: Se coordination of Pr^{3+} ions and partial/full Cl coordination of Pr^{3+} ions. In addition, simplified energy level diagrams of the Pr^{3+}ions [45–47] reveal the PL radiative decay ($^3F_3$, $^3F_4$)→$^3H_6$ (lifetime 0.21 ms, Fig. 9) encouraged by the very low phonon energy of a chloride local environment of the Pr^{3+} ions.

Table 2 collates and summarizes the experimental Pr^{3+}-doped Ge-As-Ga_1-Se glass fiber emission lifetime results found here, together with the experimental results, and calculated results from the Judd-Ofelt (J-O) modelling, of comparable Pr^{3+}-doped Ge-As-Ga-Se bulk glasses reported by Shaw *et al.* [47] and of fiber reported by Sójka *et al.* [46]. For the $^3H_5$→$^3H_4$ transition, the experimental lifetimes found here for 500 ppmw Pr^{3+}-doped Ge-As-Ga_1-Se fibers supplied by Pr^{3+}(foil), Pr^{3+}(PrI_3) and Pr^{3+}($PrCl_3$) were of 10.1 ± 0.2 ms, 10.4 ± 0.2 ms and 10.3 ± 0.7 ms, respectively, to be compared with 10.0 ms [46] to 15.0 ms [47], estimated errors ~30% [47], from J-O modelling and a measured lifetime of 12.0 ms in an unspecified 'low concentration dopant' Pr^{3+}-doped Ge-As-Ga-Se bulk glass [47] and 11.5 ms in a 115 mm long, 500 ppmw Pr^{3+}(foil)-doped Ge-As-Ga-Se fiber collected at the end of the fiber [46]; note that end-collection will probably have resulted some re-absorption to cause radiation trapping and can present longer lifetime. For the ($^3H_6$, $^3F_2$)→$^3H_5$ transition, the 500 ppmw Pr^{3+}(foil) and Pr^{3+}(PrI_3)-doped Ge-As-Ga_1-Se fibers here exhibited experimental lifetimes of 3.3 ± 0.2 ms and 3.2 ± 0.2 ms, respectively, and the Pr^{3+}($PrCl_3$)-doped Ge-As-Ga_1-Se fiber gave a slightly shorter lifetime of 2.4 ± 0.7 ms, to be comparable with a calculated lifetime of 3.4 ms and a measured lifetime of 2.7 ms in the literature [1,47]. The extra radiative lifetime of 0.21 ± 0.06 ms observed only for the Pr^{3+}($PrCl_3$)-doped Ge-As-Ga_1-Se fiber here - assigned as ($^3F_3$, $^3F_4$)→$^3H_6$, had theoretical and experimental lifetimes reported as 0.29 ms and 0.25 ms, respectively, by Shaw *et al* [47]. However, unlike in the current work, Shaw *et al.* determined

Optical Materials EXPRESS

the experimental lifetime indirectly from the decay at 1.7 μm wavelength (*i.e.* ($^3F_3$, $^3F_4$)→$^3H_4$) [47], instead of direct measurement of the transition ($^3F_3$, $^3F_4$)→$^3H_6$, as done here.

In Table 2, the lifetimes of the $PrCl_3$-doped fiber were slightly shorter in ($^3H_6$, $^3F_2$)→$^3H_5$ (2.4 ms compared to 2.7-3.4 ms) and ($^3F_3$, $^3F_4$)→$^3H_6$ (0.21 ms compared to 0.25 and 0.29 ms) (although the bigger error in lifetimes in the $PrCl_3$-doped fiber should be noted due to a lower signal-to-noise ratio), which is a hint of lifetime-quenching. Any lifetime-quenching, if it occurred, may have been due to Pr-Cl clustering in the $PrCl_3$-doped fiber. On the other hand, because lifetime quenching was not really significant in the $PrCl_3$-doped fiber, it suggests that the majority of the Pr-Cl sites were distributed more evenly instead of any clustering of Pr^{3+}. In Table 2, the lifetimes of PrI_3-doped fiber are found to be comparable with the values of the Pr-foil doped fiber, which indicates no distinct Pr^{3+} ion clustering had occurred in the PrI_3-doped fiber. This chimes with the discussion above that the sites of Pr-I coordination in the PrI_3-doped fiber were lower in number density than the Pr-Cl sites in the $PrCl_3$-doped fiber. Thus, the amount of Pr-I clustering would also have tended to be less.

Table 2. Observed PL decay lifetimes for: $^3H_5$→$^3H_4$, ($^3H_6$, $^3F_2$)→$^3H_5$ and ($^3F_3$, $^3F_4$)→$^3H_6$ in 500 ppmw Pr^{3+}(foil)-, Pr^{3+}($PrCl_3$)- and Pr^{3+}(PrI_3)-doped Ge-As-Ga_1-Se fibers, together with calculated and experimental literature values. All samples were Pr^{3+}-doped Ge-As-Ga-Se glass hosts.

Transition	Sample form	J-O calculated lifetime / ms	Experimental lifetime / ms	Ref.
$^3H_5$→$^3H_4$	Pr, bulk	15.0	12.0	[47][a]
	Pr foil, fiber	10.0	11.5	[46]
	Pr foil, fiber	-	10.1	This work
	PrI_3, fiber	-	10.4	
	$PrCl_3$, fiber	-	10.3	
($^3H_6$, $^3F_2$)→$^3H_5$	Pr, bulk	3.4	2.7[b]	[1,47][a]
	Pr foil, fiber	-	3.3	This work
	PrI_3, fiber	-	3.2	
	$PrCl_3$, fiber	-	2.4	
($^3F_3$, $^3F_4$)→$^3H_6$	Pr, bulk	0.29	0.25[c]	[47][a]
	Pr foil, fiber	-	-	This work
	PrI_3, fiber	-	-	
	$PrCl_3$, fiber	-	0.21	

[a]State of Pr in additive is not given in [47].

[b]Two experimental values (2.7 ms and 4.2 ms) found for ($^3H_6$, $^3F_2$)→$^3H_5$ in [47] and according to [1] it is confirmed to be 2.7 ms.

[c]Inferred from measurement at 1.7 μm wavelength (($^3F_3$, $^3F_4$)→$^3H_4$).

In comparison with the modeling work on Pr^{3+} -doped chalcogenide glass MIR fiber amplifiers/lasers in recent years (2015-2018) [1, 2, 29, 31, 32], the measured lifetimes of 10.1-10.4 ms of $^3H_5$, 2.4-3.3 ms of ($^3H_6$, $^3F_2$) and 0.21 ms of ($^3F_3$, $^3F_4$), respectively, in this work are comparable with the lifetimes of 6.5-12.2 ms of $^3H_5$ [1,2,29,31,32], 2.7-4.56 ms of ($^3H_6$, $^3F_2$) [1, 31, 32] and 0.1 ms of ($^3F_3$, $^3F_4$) [2], respectively, used in published modeling work. This indicates that the Pr^{3+} -doped glass fiber system of this work has the potential to be developed into fiber amplifiers and/or lasers. However, the optical fiber loss of this work (~30 dB/m at 4.5 μm wavelength, due to the Se-H contamination band) is much higher than the losses used in the modelling work, where the optical loss assumed is generally 1 dB/m [1, 29, 31, 32], or 3-7 dB/m [2, 31, 32] for signal wavelengths of 4.3-5.0 μm. The optical loss is a key issue that presently prevents the realization of MIR fiber amplification and lasing in chalcogenide glasses, and is an important research challenge to be solved.

Optical Materials EXPRESS

4. Conclusions

The work presents a comparative study of 500 ppmw Pr^{3+} (introduced by Pr foil, PrI_3 or $PrCl_3$ additive) doped Ge-As-Ga_1-Se glass fibers. No crystallization peak was found in powder XRD patterns of any of the Pr^{3+}-doped fibers. Fiber loss spectra showed that the Pr(foil)-doped fiber had the lowest overall background optical loss of ~2.0-2.5 dB/m across the 2-9 μm window. Although the $PrCl_3$-doped fiber presented excess NIR scattering loss below 4 μm wavelength, it gave the lowest loss of all doped fibers here of 1.8 dB/m at 6.9 μm wavelength. Excess NIR scattering loss was also observed in the PrI_3-doped fiber below 4 μm wavelength but lower than that of the $PrCl_3$-doped fiber. FTIR spectra of the preform bulk glass (*i.e.* the glass before fiber drawing) showed that most of the extra NIR scattering loss in the PrI_3-doped and $PrCl_3$-doped fibers was already in the preforms due to RE additive solubility and not caused by crystallization from fiber-drawing; in addition, structured Pr^{3+} absorption bands were present in FTIR spectra of the PrI_3- and $PrCl_3$- doped Ge-As-Ga_1-Se preforms.

PL spectra and lifetimes under 1550 nm pumping of the Pr^{3+}-doped Ge-As-Ga_1-Se fibers showed reproducibly that PL intensity at 4700 nm wavelength was in the order: Pr(foil)-doped fiber > PrI_3-doped fiber > $PrCl_3$-doped fiber. The PL intensity at 4700 nm wavelength of all doped fibers, increased with a gentle sublinear behavior (proposed due to ground state bleaching), as incident pump power increased. The Pr^{3+}-doped fibers had radiative lifetimes of 10.1-10.4 ms for the transition of $^3H_5 \rightarrow {}^3H_4$, and 2.4-3.3 ms for the transition of $(^3H_6, {}^3F_2) \rightarrow {}^3H_5$. The local Pr^{3+} ions environment in the $PrCl_3$-doped fiber was suggested to have at least a portion of Pr-Cl to account for the extra 0.21 ms radiative lifetime found for the transition of $(^3F_3, {}^3F_4) \rightarrow {}^3H_6$, but not observed in the Pr(foil) and PrI_3-doped fibers. The content of Ga required to solubilize the same amount of Pr^{3+} ions is suggested to be in order of: $Ga_{PrCl3} > Ga_{PrI3} > Ga_{Pr\text{-}foil}$, and future work can be carried out to study the optimum Ga ratio for REI_3 and $RECl_3$ dopants, along with future investigation by glass structural experiments (*e.g.* high intensity X-ray diffraction) and a thermal analysis with microscopy study. Also, the preparation of high purity rare earth ion doped chalcogenide glass fiber continues to be a vital research direction.

Funding

EPSRC (EP/P013708/1); European Commission (317803).

Acknowledgment

This work was supported by the Engineering and Physical Sciences Research Council [grant number EP/P013708/1] through project COOL (COld-cOntainer processing for Long-wavelength mid-infrared fibreoptics) and the European Commission through Framework Seven (FP7) project MINERVA (MId- to NEaR infrared spectroscopy for improVed medical the diAgnostics; 317803).

References

1. J. Hu, C. R. Menyuk, C. Wei, L. Brandon Shaw, J. S. Sanghera, and I. D. Aggarwal, "Highly efficient cascaded amplification using Pr^{3+}-doped mid-infrared chalcogenide fiber amplifiers," Opt. Lett. **40**(16), 3687–3690 (2015).
2. E. A. Anashkina, "Design and numerical modeling of broadband mid-IR rare-earth-doped chalcogenide fiber amplifiers," IEEE Photonics Technol. Lett. **30**(13), 1190–1193 (2018).
3. F. Starecki, F. Charpentier, J.-L. Doualan, L. Quetel, K. Michel, R. Chahal, J. Troles, B. Bureau, A. Braud, P. Camy, V. Moizan, and V. Nazabal, "Mid-IR optical sensor for CO_2 detection based on fluorescence absorbance of Dy^{3+}:$Ga_5Ge_{20}Sb_{10}S_{65}$ fibers," Sens. Actuators B Chem. **207**, 518–525 (2015).
4. A. L. Pelé, A. Braud, J. L. Doualan, F. Starecki, V. Nazabal, R. Chahal, C. Boussard-Plédel, B. Bureau, R. Moncorgé, and P. Camy, "Dy^{3+} doped GeGaSbS fluorescent fiber at 4.4 μm for optical gas sensing: comparison of simulation and experiment," Opt. Mater. **61**, 37–44 (2016).
5. F. Starecki, S. Morais, R. Chahal, C. Boussard-Plédel, B. Bureau, F. Palencia, C. Lecoutre, Y. Garrabos, S. Marre, and V. Nazabal, "IR emitting Dy^{3+} doped chalcogenide fibers for in situ CO_2 monitoring in high pressure microsystems," Int. J. Greenh. Gas Control **55**, 36–41 (2016).

Optical Materials EXPRESS

6. A. B. Seddon, "Chalcogenide glasses: a review of their preparation, properties and applications," J. Non-Cryst. Solids **184**(0), 44–50 (1995).
7. S. D. Jackson, "Towards high-power mid-infrared emission from a fibre laser," Nat. Photonics **6**(7), 423–431 (2012).
8. W. H. Kim, V. Q. Nguyen, L. B. Shaw, L. E. Busse, C. Florea, D. J. Gibson, R. R. Gattass, S. S. Bayya, F. H. Kung, G. D. Chin, R. E. Miklos, I. D. Aggarwal, and J. S. Sanghera, "Recent progress in chalcogenide fiber technology at NRL," J. Non-Cryst. Solids **431**, 8–15 (2016).
9. V. S. Shiryaev, E. V. Karaksina, T. V. Kotereva, M. F. Churbanov, A. P. Velmuzhov, M. V. Sukhanov, L. A. Ketkova, N. S. Zernova, V. G. Plotnichenko, and V. V. Koltashev, "Preparation and investigation of Pr^{3+}-doped Ge–Sb–Se–In–I glasses as promising material for active mid-infrared optics," J. Lumin. **183**, 129–134 (2017).
10. R. S. Quimby, L. B. Shaw, J. S. Sanghera, and I. D. Aggarwal, "Modeling of cascade lasing in Dy^{3+} chalcogenide glass fiber laser with efficient output at 4.5 microns," IEEE Photonics Technol. Lett. **20**(2), 123–125 (2008).
11. Ł. Sójka, Z. Tang, H. Zhu, E. Beres-Pawlik, D. Furniss, A. B. Seddon, T. M. Benson, and S. Sujecki, "Study of mid-infrared laser action in chalcogenide rare earth doped glass with Dy^{3+}, Pr^{3+} and Tb^{3+}," Opt. Mater. Express **2**(11), 1632–1640 (2012).
12. M. C. Falconi, G. Palma, F. Starecki, V. Nazabal, J. Troles, S. Taccheo, M. Ferrari, and F. Prudenzano, "Design of an efficient pumping scheme for mid-IR Dy^{3+}:$Ga_5Ge_{20}Sb_{10}S_{65}$ PCF fiber laser," IEEE Photonics Technol. Lett. **28**(18), 1984–1987 (2016).
13. X. Xiao, Y. Xu, H. Guo, P. Wang, X. Cui, M. Lu, Y. Wang, and B. Peng, "Theoretical modeling of 4.3 μm mid-infrared lasing in Dy^{3+}-doped chalcogenide fiber lasers," IEEE Photonics J. **10**(2), 1–11 (2018).
14. A. Galstyan, S. H. Messaddeq, V. Fortin, I. Skripachev, R. Vallée, T. Galstian, and Y. Messaddeq, "Tm^{3+} doped Ga-As-S chalcogenide glasses and fibers," Opt. Mater. **47**, 518–523 (2015).
15. Z. Tang, D. Furniss, M. Fay, N. C. Neate, Y. Cheng, E. Barney, L. Sojka, S. Sujecki, T. M. Benson, and A. B. Seddon, "First identification of rare-earth oxide nucleation in chalcogenide glasses and implications for fabrication of mid-infrared active fibers," J. Am. Ceram. Soc. **97**(2), 432–441 (2014).
16. Z. Tang, N. C. Neate, D. Furniss, S. Sujecki, T. M. Benson, and A. B. Seddon, "Crystallization behavior of Dy^{3+}-doped selenide glasses," J. Non-Cryst. Solids **357**(11–13), 2453–2462 (2011).
17. Y. Huang, Z. Liu, H. Chen, J. Bian, X. Zhang, X. Wang, and S. Dai, "Research on structure and mid-infrared photoluminescence of Ga^{3+}/Er^{3+} co-doped As-S glasses," J. Non-Cryst. Solids **471**, 456–461 (2017).
18. Z. Tang, D. Furniss, N. C. Neate, E. Barney, T. M. Benson, and A. B. Seddon, "Dy^{3+}-doped selenide chalcogenide glasses: influence of Dy^{3+} dopant-additive and containment," J. Am. Ceram. Soc. **99**(7), 2283–2291 (2016).
19. W. J. Chung, H. S. Seo, B. J. Park, J. T. Ahn, and Y. G. Choi, "Selenide glass optical fiber doped with Pr^{3+} for U-band optical amplifier," ETRI J. **27**(4), 411–417 (2005).
20. B. J. Park, H. S. Seo, J. T. Ahn, Y. G. Choi, D. Y. Jeon, and W. J. Chung, "Mid-infrared (3.5-5.5 μm) spectroscopic properties of Pr^{3+}-doped Ge-Ga-Sb-Se glasses and optical fibers," J. Lumin. **128**(10), 1617–1622 (2008).
21. M. Zhang, A. Yang, Y. Peng, B. Zhang, H. Ren, W. Guo, Y. Yang, C. Zhai, Y. Wang, Z. Yang, and D. Tang, "Dy^{3+}-doped Ga–Sb–S chalcogenide glasses for mid-infrared lasers," Mater. Res. Bull. **70**, 55–59 (2015).
22. E. R. Barney, Z. Tang, A. Seddon, D. Furniss, S. Sujecki, T. Benson, N. Neate, and D. Gianolio, "The local environment of Dy^{3+} in selenium-rich chalcogenide glasses," RSC Advances **4**(80), 42364–42371 (2014).
23. Z. Tang, D. Furniss, M. Fay, N. C. Neate, S. Sujecki, T. M. Benson, and A. B. Seddon, "Crystallisation and optical loss studies of Dy^{3+}-doped, low Ga content, selenide chalcogenide bulk glasses and optical fibers," in *Processing, Properties, and Applications of Glass and Optical Materials: Ceramic Transactions*, A. K. Varshneya, H. A. Schaeffer, K. A. Richardson, M. Wightman, and L. D. Pye, eds. (John Wiley & Sons, Inc., Hoboken, NJ, USA, 2012), pp. 193–199.
24. A. P. Velmuzhov, A. A. Sibirkin, V. S. Shiryaev, and M. F. Churbanov, "Equilibrium in GeI_4-S(Se) systems," J. Optoelectron. Adv. Mater. **13**(11–12), 1437–1441 (2011).
25. A. P. Velmuzhov, A. A. Sibirkin, V. S. Shiryaev, M. F. Churbanov, A. I. Suchkov, A. M. Potapov, R. M. Shaposhnikov, V. G. Plotnichenko, and V. V. Koltashev, "Preparation of Ge-Sb-S-I glass system via volatile iodides," J. Optoelectron. Adv. Mater. **13**(8), 936–939 (2011).
26. E. V. Karaksina, V. S. Shiryaev, T. V. Kotereva, A. P. Velmuzhov, L. A. Ketkova, and G. E. Snopatin, "Preparation of high-purity Pr^{3+} doped Ge–As–Se–In–I glasses for active mid-infrared optics," J. Lumin. **177**, 275–279 (2016).
27. E. V. Karaksina, V. S. Shiryaev, T. V. Kotereva, and M. F. Churbanov, "Preparation of high-purity Pr(3+) doped Ge–Ga–Sb–Se glasses with intensive middle infrared luminescence," J. Lumin. **170**, 37–41 (2016).
28. V. S. Shiryaev, A. P. Velmuzhov, Z. Q. Tang, M. F. Churbanov, and A. B. Seddon, "Preparation of high purity glasses in the Ga–Ge–As–Se system," Opt. Mater. **37**(0), 18–23 (2014).
29. E. V. Karaksina, V. S. Shiryaev, M. F. Churbanov, E. A. Anashkina, T. V. Kotereva, and G. E. Snopatin, "Core-clad Pr(3+)-doped Ga(In)-Ge-As-Se-(I) glass fibers: preparation, investigation, simulation of laser characteristics," Opt. Mater. **72**, 654–660 (2017).
30. Q. Guo, Y. Xu, H. Guo, X. Xiao, C. Lin, X. Cui, P. Wang, F. Gao, M. Lu, and B. Peng, "Effect of iodine (I_2) on structural, thermal and optical properties of Ge-Sb-S chalcohalide host glasses and ones doped with Dy," J. Non-Cryst. Solids **464**, 81–88 (2017).
31. M. A. Khamis, R. Sevilla, and K. Ennser, "Large mode area Pr^{3+}-doped chalcogenide PCF design for high efficiency mid-IR laser," IEEE Photonics Technol. Lett. **30**(9), 825–828 (2018).

Optical Materials EXPRESS

32. L. Sójka, Z. Tang, D. Furniss, H. Sakr, E. Bereś-Pawlik, A. B. Seddon, T. M. Benson, and S. Sujecki, "Numerical and experimental investigation of mid-infrared laser action in resonantly pumped Pr^{3+} doped chalcogenide fibre," Opt. Quantum Electron. **49**(1), 21 (2017).
33. Z. Tang, D. Furniss, N. C. Neate, T. M. Benson, and A. B. Seddon, "Low gallium-content, dysprosium III doped, Ge-As-Ga-Se chalcogenide glasses for active mid-infrared fiber optics," J. Am. Ceram. Soc. **0**(0), 1–12 (2018).
34. B. G. Aitken, C. W. Ponader, and R. S. Quimby, "Clustering of rare earths in GeAs sulfide glass," C. R. Chim. **5**(12), 865–872 (2002).
35. J. K. Kim, B. K. Jin, W. J. Chung, B. J. Park, J. Heo, and Y. G. Choi, "Influence of the Ga addition on optical properties of Pr in Ge-Sb-Se glasses," J. Phys. Chem. Solids **72**(11), 1386–1389 (2011).
36. T. H. Lee, S. I. Simdyankin, J. Hegedus, J. Heo, and S. R. Elliott, "Spatial distribution of rare-earth ions and GaS_4 tetrahedra in chalcogenide glasses studied via laser spectroscopy and ab initio molecular dynamics simulation," Phys. Rev. B Condens. Matter Mater. Phys. **81**(10), 104204 (2010).
37. Z. Tang, V. S. Shiryaev, D. Furniss, L. Sojka, S. Sujecki, T. M. Benson, A. B. Seddon, and M. F. Churbanov, "Low loss Ge-As-Se chalcogenide glass fiber, fabricated using extruded preform, for mid-infrared photonics," Opt. Mater. Express **5**(8), 1722–1737 (2015).
38. O. Henderson-Sapir, J. Munch, and D. J. Ottaway, "New energy-transfer upconversion process in Er^{3+}:ZBLAN mid-infrared fiber lasers," Opt. Express **24**(7), 6869–6883 (2016).
39. H. Sakr, D. Furniss, Z. Tang, L. Sojka, N. A. Moneim, E. Barney, S. Sujecki, T. M. Benson, and A. B. Seddon, "Superior photoluminescence (PL) of Pr^{3+}-In, compared to Pr^{3+}-Ga, selenide-chalcogenide bulk glasses and PL of optically-clad fiber," Opt. Express **22**(18), 21236–21252 (2014).
40. A. B. Seddon, D. Furniss, Z. Q. Tang, S. Ł. T. M. Benson, R. Caspary, and S. Sujecki, "True mid-infrared Pr^{3+} absorption cross-section in a selenide-chalcogenide host-glass," in *2016 18th International Conference on Transparent Optical Networks (ICTON)* (2016), pp. 1–6.
41. M. E. Lines, "Scattering losses in optic fiber materials. II. Numerical estimates," J. Appl. Phys. **55**(11), 4058–4063 (1984).
42. M. Churbanov, G. Snopatin, V. Shiryaev, V. Plotnichenko, and E. Dianov, "Recent advances in preparation of high-purity glasses based on arsenic chalcogenides for fiber optics," J. Non-Cryst. Solids **357**(11), 2352–2357 (2011).
43. G. E. Snopatin, V. S. Shiryaev, V. G. Plotnichenko, E. M. Dianov, and M. F. Churbanov, "High-purity chalcogenide glasses for fiber optics," Inorg. Mater. **45**(13), 1439–1460 (2009).
44. H. Sakr, Z. Tang, D. Furniss, L. Sojka, S. Sujecki, T. M. Benson, and A. B. Seddon, "Promising emission behavior in Pr^{3+}/In selenide-chalcogenide-glass small-core step index fiber (SIF)," Opt. Mater. **67**, 98–107 (2017).
45. G. H. Dieke and H. M. Crosswhite, "The spectra of the doubly and triply ionized rare earths," Appl. Opt. **2**(7), 675–686 (1963).
46. L. Sójka, Z. Tang, D. Furniss, H. Sakr, A. Oladeji, E. Bereś-Pawlik, H. Dantanarayana, E. Faber, A. B. Seddon, T. M. Benson, and S. Sujecki, "Broadband, mid-infrared emission from Pr^{3+} doped GeAsGaSe chalcogenide fiber, optically clad," Opt. Mater. **36**(6), 1076–1082 (2014).
47. L. B. Shaw, B. Cole, P. A. Thielen, J. S. Sanghera, and I. D. Aggarwal, "Mid-wave IR and long-wave IR laser potential of rare-earth doped chalcogenide glass fiber," IEEE J. Quantum Electron. **37**(9), 1127–1137 (2001).
48. M. J. Weber, "Spontaneous Emission Probabilities and Quantum Efficiencies for Excited States of Pr^{3+} in LaF_3," J. Chem. Phys. **48**(10), 4774–4780 (1968).
49. L. Shaw, B. Harbison, B. Cole, J. Sanghera, and I. Aggarwal, "Spectroscopy of the IR transitions in Pr^{3+} doped heavy metal selenide glasses," Opt. Express **1**(4), 87–96 (1997).
50. S. R. Bowman, J. Ganem, B. J. Feldman, and A. W. Kueny, "Infrared laser characteristics of praseodymium-doped lanthanum trichloride," IEEE J. Quantum Electron. **30**(12), 2925–2928 (1994).
51. M. Velázquez, A. Ferrier, J.-L. Doualan, and R. Moncorgé, "Rare-earth-doped low phonon energy halide crystals for mid-infrared laser sources," in *Solid State Laser* (InTech, 2012), pp. 119–142.
52. B. Cole, L. B. Shaw, P. C. Pureza, R. Mossadegh, J. S. Sanghera, and I. D. Aggarwal, "Rare-earth doped selenide glasses and fibers for active applications in the near and mid-IR," J. Non-Cryst. Solids **256–257**, 253–259 (1999).
53. Z. Liu, J. Bian, Y. Huang, T. Xu, X. Wang, and S. Dai, "Fabrication and characterization of mid-infrared emission of Pr^{3+} doped selenide chalcogenide glasses and fibres," RSC Advances **7**(66), 41520–41526 (2017).
54. A. B. Seddon and M. A. Hemingway, "Thermal properties of chalcogenide-halide glasses in the system: Ge-S-I," J. Therm. Anal. **37**(9), 2189–2203 (1991).